Chapter 8
Comprehensive Assessment of Aortopathy Using Catheterization

Hirofumi Saiki and Hideaki Senzaki

Abstract Aortopathy is represented by aortic wall histological alterations, which are translated into alterations of mechanical property of the aortic wall. Because aortic pressure waveform in itself contains comprehensive information about aortic wall mechanical property, analysis of aortic pressure waveform either alone or coupled with aortic flow provides important diagnostic and therapeutic information about aortopathy. Catheter examination is the only way to precisely obtain the aortic waveform and thus plays an independent role compared to numerous noninvasive imaging modalities, such as echocardiogram, computed tomography, and magnetic resonance imaging. In this chapter, we summarize our knowledge about the aortic wall mechanical properties in several forms of aortopathy elegantly assessed by catheter examination.

Keywords Mechanical property • Pulse wave velocity • Impedance • Wave intensity • Wave reflection • Pressure–volume relationship

8.1 Introduction

Although the advancement of imaging technology has greatly contributed to the better understanding of hemodynamics in a variety of cardiac diseases, cardiovascular pressure waveform is still a fundamental factor that well characterizes cardiovascular properties. Invasive catheter insertion is the only method for obtaining actual pressure waveform in a specific location of the cardiovascular system, and the utility of alternative methods, such as applanation tonometry or MRI, has not yet been fully validated to estimate actual pressure waveform for patients with cardiovascular diseases [1, 2]. Pathology of the tunica media of the aortic wall is reportedly responsible for the onset of aortopathy in congenital or acquired cardiovascular diseases [3, 4], and hemodynamic stress as well as genetic backgrounds can induce it by activating inflammatory cascade and tissue permeability, which is

H. Saiki, M.D. • H. Senzaki, M.D. (✉)
Department of Pediatric Cardiology, Saitama Medical Center, Saitama Medical University, Room 415, Staff Office Building, 1981 Kamoda, Kawagoe, Saitama 350-8550, Japan
e-mail: hsenzaki@saitama-med.ac.jp

K. Niwa, H. Kaemmerer (eds.), *Aortopathy*, DOI 10.1007/978-4-431-56071-5_8

called mechanotransduction [5–11]. Accumulating evidence elucidated that intravascular blood pressure flow dynamics are closely related to the molecular mechanisms of the evolving aortopathy, particularly in patients with structural heart diseases [7, 10, 12, 13]. Accordingly, a precise understanding of cardiovascular mechanical properties and their interaction with aortic hemodynamics may allow us to identify optimal hemodynamic management that may ameliorate the clinical course of aortopathy, even under the significant influence of genetic factors. Thus, catheter examination has advantages over noninvasive assessments in terms of understanding the pathophysiology of aortopathy. This further understanding will contribute to the improvement of current hemodynamic management.

8.2 Aortic Hemodynamics and Pathology (Fig. 8.1, Details in Chaps. 2 and 3)

Elastic fiber disruption and fatigue of aortic tunica media are fundamental pathologies of the aortic dilatation in aortopathy. Although the elastic fibers in the aorta are considered to tolerate pulsatile stress by an intermittent ventricular ejection for more than decades [14], early disruption can be induced by inflammation or

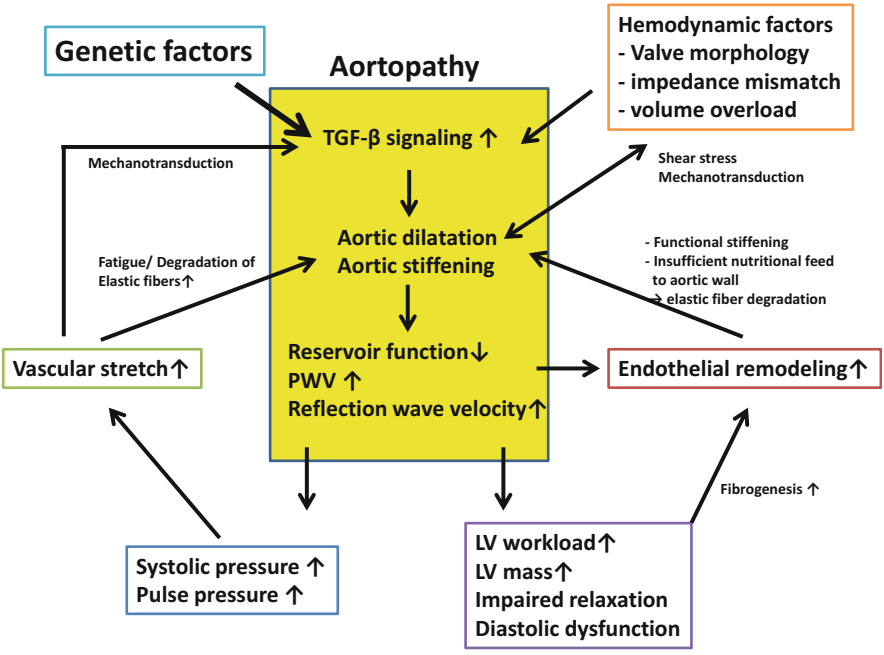

Fig. 8.1 Mechanisms for developing aortic dilatation

perturbation of the protein maintenance system, which is regulated by local gene expression [15, 16]. Although Marfan syndrome is the typical systemic disease that causes accelerated degradation of the aortic elastic fibers, mainly due to gene mutation encoding microfibril protein, fibrillin-1 [15, 17], similar pathology of the tunica media is also observed in patients with congenital heart disease, including bicuspid aortic valve, tetralogy of Fallot (TOF), and others [4]. Not limited to genetic factors or direct surgical vascular insults, characteristic hemodynamics such as excessive volume overload, augmented pressure load, or accelerated blood velocity induce vascular stress that activates inflammatory gene expression via mechanotransduction [10]. Mounting evidence has suggested a significant contribution of hemodynamics to the development of aortopathy [5, 7, 12]. Vascular mechanical stress, which can affect the aortic structure, mainly consists of normal stress and shear stress. Normal stress, which represents excessive vascular stretch, induces alteration of myosin–actin interaction and conformational changes of its linker proteins. Interaction with integrin, which connects the endothelial myosin–actin complex and extracellular matrix, ultimately stimulates TGF-β production, its release, and cellular growth [10]. When vascular endothelium senses an increase in shear stress, which is determined by both blood viscosity and blood flow velocity, relaxation of medial smooth muscle compensates to decrease it. Although shear stress regulates vascular dilatation in conductance arteries [18, 19], it also promotes endothelial permeability [20], proliferation of endothelial cells, and aortic remodeling [12]. A stiffened arterial system due to remodeling increases pulse pressure and ventricular afterload [21]. In addition, aortic remodeling decreases nutritional feed to the aortic wall from the aortic cavity, making it more dependent on the vasa vasorum, resulting in malnutrition of the tunica media. As reported by Stefanadis, the decrease of the aortic wall blood feed by removal of the vasa vasorum resulted in acute tunica media degradation and increased stiffness [22], suggesting a fundamental role of blood feeding for the maintenance of the tunica media. This is also supported by the fact that improper perfusion of the vasa vasorum relates to aortic wall stiffness [23]. Thus, degradation of the aortic tunica media is initiated by combined effects from inflammatory responses, pressure augmentation, and insufficient aortic wall blood supply; then, the aortic wall starts to dilate by a loss of elastic fibers. Eventually, the aortic wall becomes predominantly supported by the collagens, which are much stiffer than elastic fibers, and the characteristic features of aortopathy, including aortic dilatation and stiffness, are constructed. Accordingly, management of hemodynamics might be fundamentally important in preventing the development of aortopathy, because aortic mechanical stress is determined by blood pressure, velocity, and viscosity, which are factors of cardiac output, vascular resistance, and oxygen saturation.

8.3 Impedance Mismatch

Characteristic features of aortopathy, including augmented stiffness, aortic dilatation, and subsequent distal narrowing, result in heterogeneity of aortic properties, both in histological feature and aortic diameter. Although energy transmission between two locations of the vessel is maximized if the vascular property is uniform (known as impedance match), part of the blood energy can reflect at any part of the vessel and increase proximal input impedance if a vascular property difference exists [24–26]. In normal circulation, discontinuity of vascular properties in the peripheral arterial system, including relative narrowing and higher stiffness of the peripheral artery compared to that of the aorta, prevents end organs from exposure to high systolic blood energy by reflecting part of the energy. At the same time, it preserves redundant energy in the aortic wall as potential energy so that blood can be delivered to peripheral organs evenly during diastole [27]. In contrast, if central aortic stiffness becomes close to the level of that in peripheral arteries, then more pulsatile energy is delivered to the end organs and can impair their function [28, 29]. This also decreases reserved energy of the aorta, leading to decreased diastolic blood flow. Such discontinuity of vascular properties is called "impedance mismatch," and this can also accelerate the onset as well as progress of aortopathy by improper augmentation of proximal aortic waveform (Fig. 8.2). In addition to affecting the aorta and systemic circulation, an arising reflection wave in the proximal part of the aorta can be an additional ventricular afterload [21] and can impair ventricular function as well as myocardial energetic efficiency by affecting ventricular–arterial (VA) coupling [30, 31].

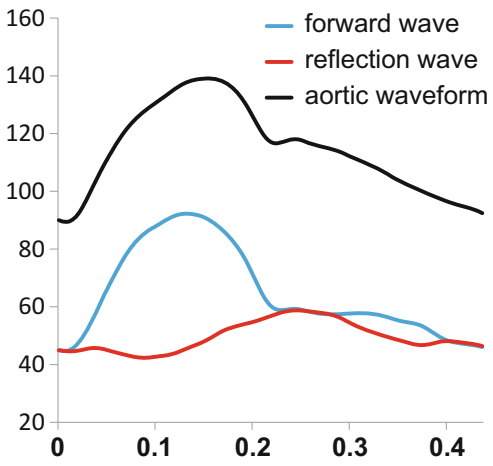

Fig. 8.2 Aortic pressure waveform consists of forward and backward pressure flows. The aortic pressure waveform can be factorized into forward-traveling flow and backward flow [44, 45]

8.4 Practical Utility of the Catheter Examination in Aortopathy

Although the shapes of the aorta are easily recognized using MRI or other imaging modalities of three-dimensional images, cardiovascular contrast imaging during catheter examination is two-dimensional and angle dependent, so its utility for morphological assessment is considerably limited in the current era. Meanwhile, having actual pressure waveform is a significant advantage in the assessment of vascular properties in catheter assessment. Catheter examination is commonly performed in patients with congenital heart diseases, so being conversant with such methods would highly support logical decision-making in the clinical setting.

8.4.1 Pulse Wave Velocity

One simple but reliable index for arterial stiffness assessed by catheter examination is pulse wave velocity (PWV). The American Heart Association identified PWV as a noninvasive and reliable marker of aortic stiffness [32]. Although noninvasive PWV is widely used in the clinical setting, PWV is also available during cardiac catheterization. During catheter drawback in the aorta, wave traveling distance is easily obtained by measuring the catheter extraction distance. The time gaps from the ECG R wave to the upstroke of aortic pressure at the starting point and at the end point of extraction represent wave traveling time. Thus, PWV can be calculated as extraction distance divided by wave traveling time [33]. As represented by the Moens–Korteweg equation (Eq. 8.1), PWV increases with the stiffening of the vascular wall, assuming that both vascular wall thickness and vessel area are almost the same.

$$\mathrm{PWV} = \left(\sqrt{E}*\sqrt{h}\right)/\left(\sqrt{\rho}*\sqrt{D}\right) \tag{8.1}$$

where E is Young's modules, h is vascular wall thickness, ρ is blood density, and D is vessel radius diameter. PWV is a predictor of cardiovascular events in heart failure or ischemic heart disease [34, 35]. Higher PWV is reported in patients with Marfan syndrome regardless of aortic dilatation [36], suggesting a possible relationship between PWV and histological change of the tunica media, as well as the predictive value for future aortopathy [37]. As represented in Eq. 8.1, PWV should theoretically decrease with the increase of aortic diameter. Accordingly, the increase of PWV in the dilated aorta further highlights significant stiffening of the aorta. In sharp contrast, PWV in bicuspid aortic valve patients without aortic dilatation was similar to that in tricuspid valve patients [38]. Even though PWV and arterial elastance were similar, aortic wall shear rate was significantly higher in bicuspid aortic valve patients than in tricuspid valve patients [38]. Although

prospective observation is required, this result implies a significant contribution of hemodynamics.

We also reported increased aortic stiffness using catheter-based PWV in tetralogy of Fallot (TOF) both before and after anatomical repair compared to control patients [5, 39]. This trend was rather similar to that of Marfan syndrome, and it also implies the possible contribution of genetic factors for the development of aortopathy in TOF. Increased aortic stiffness was also observed in patients with a single ventricular heart, with close correlation with diameter of the ascending aorta [40]. Together, PWV can be a potential predictor for aortopathy, and it may also relate to aortic medial histology. Although those analyses might have been performed even with noninvasive methods [41, 42], catheter assessment allows the consideration of vascular morphological variety, which cannot be assessed with noninvasive methods. More importantly, aortic stiffness in a specific segment is also available if catheter-based PWV is utilized. In TOF patients, ascending aortic stiffness was significantly heightened, whereas that of descending aortic stiffness was not augmented, consistent with the reported distribution of tunica media degradation in similar patient cohorts [3, 43]. Because this method allows us to use PWV of the descending aorta as the internal control, catheter-based PWV is anticipated to be applied to a wide range of cardiovascular conditions.

8.4.2 Assessment of Blood Pressure Waveforms

The other advantage of invasive catheter examination is the availability of a blood pressure waveform at any site of the vessel. Pressure waveform consists of the sum of a forward-traveling pressure wave and a reflected wave (Fig. 8.2) [44, 45]. PWV increases with aortic stiffening, thus allowing the reflection wave to overlap earlier on the subsequent forward pressure wave in the proximal aorta. Because the local blood pressure waveform can be affected by any vascular property change (impedance mismatch) from the distal part of vessel, its morphology identifies how caliber change or stiffness change alters the actual blood pressure waveform. The augmentation index (AI), which is calculated as the augmentation pressure divided by pulse pressure, is the index of the vascular property found by observing the arrival of the wave reflex at a specific site (Fig. 8.3) [46]. Although AI can be affected by the length of the aorta (i.e., patient's height), heart rate, or cardiac output due to its innate nature, patients with a bicuspid aortic valve were reported to have increased aortic stiffness and high AI, both of which were correlated with aortic dilatation [8], suggesting aortopathy as the source of pressure augmentation. Lee et al. investigated AI using applanation tonometry in bicuspid aortic valve patients and revealed close correlation with E/e′ [47]. Because increased afterload can be a predisposing factor for ventricular stiffening [31], its finding endorses the impact of aortopathy to exert afterload that relates to the reflection wave. Together, the aortic pressure waveform might be a feasible index to determine VA interaction for patients with aortopathy.

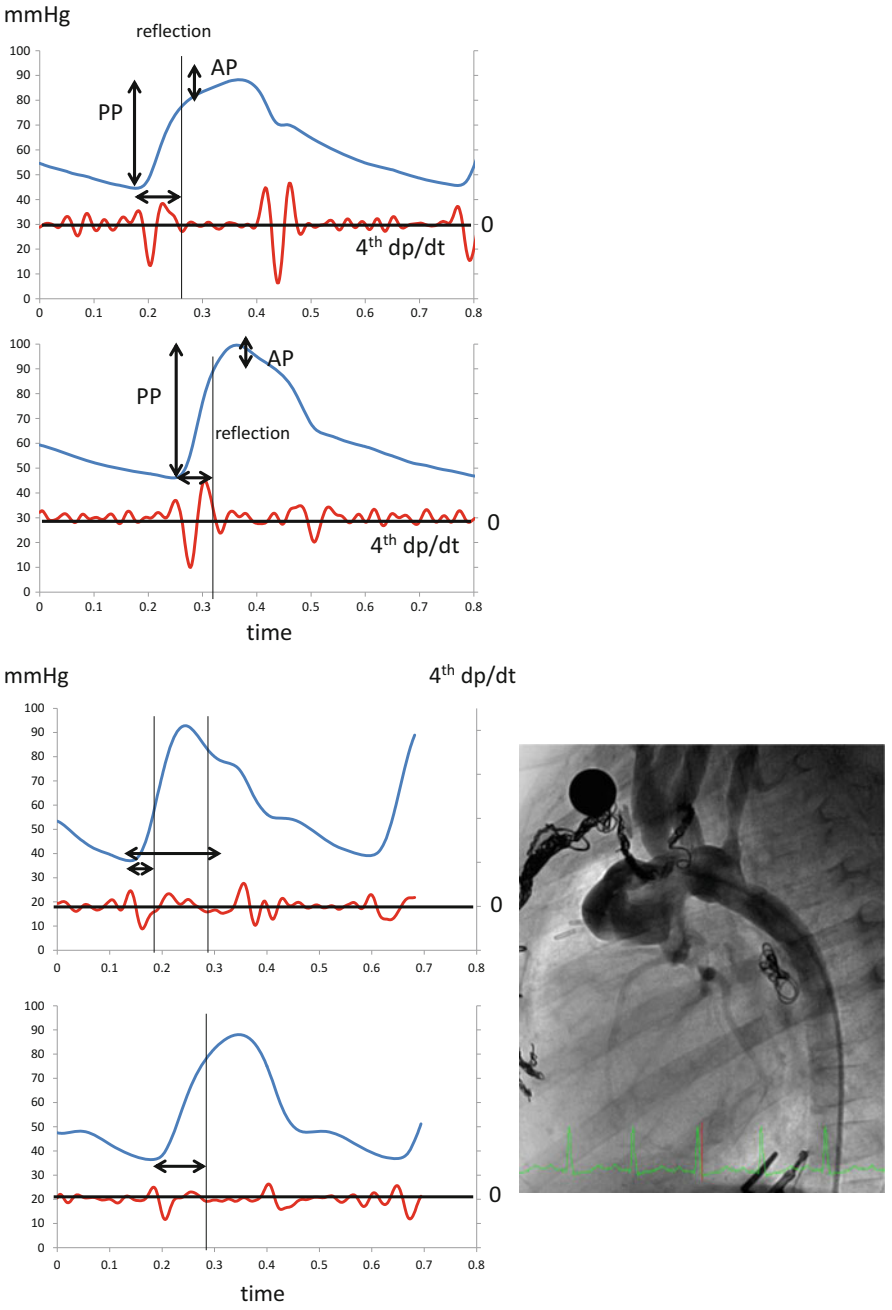

Fig. 8.3 Identification of pressure augmentation. *AP* augmentation pressure, *PP* pulse pressure. The onset of pressure augmentation by reflection (Ri) was identified by the fourth differentiate of the pressure waveform (Kelly et al.) [73]. (**a**) *Upper panel*: Ascending aortic pressure waveform in a patient with a normal aortic arch. The time interval between upstroke of pressure and Ri in the ascending aorta is relatively long, and peak aortic pressure is close to the time of dicrotic notch, allowing higher diastolic pressure. This is suitable for maximizing coronary driving pressure.

Pressure assessment using invasive catheterization is increasing its utility in the assessment of aortopathy. The case report published by Murakami et al. suggested aortopathy as a possible source of supra vena cava (SVC) stenosis [48]. Because SVC is a compliant vein and is considered to be durable against compression in general, we need to carefully interpret this case regarding whether surgical scars and postoperative adhesions associated with SVC/aortic cannulation contributed to functional stenosis of SVC pressure. Even with such limitations, catheter insertion is helpful for understanding whether morphological stenosis is hemodynamically problematic, particularly in a lesion where echocardiogram assessment can be inaccurate. Because SVC pressure can affect cerebral circulation [42, 49], assessment of SVC compression and its hemodynamic impact might be of further importance in preventing neurodevelopment or onset of dementia in patients with aortopathy.

8.4.3 Subendocardial Viability Ratio

Due to surgical scars or aortic caliber changes originating from specific operations (i.e., Norwood procedure or Damus–Kaye–Stansel procedure), aortic stiffness or aortic input impedance can be diverse in congenital heart diseases. A similar caliber change is observed in patients with aortopathy even without operation, and the bicuspid aortic valve is often complicated with complex heart diseases. Increased aortic stiffness is a burden for heart failure due to augmented afterload [50], and it also impairs coronary blood flow [51]. This is due to increased ventricular oxygen demand and decreased coronary arterial blood supply, as represented by augmented tension time index (TTI) and decreased diastolic time index (DTI), respectively [52]. Although the subendocardial viability ratio (SEVR) [53] is the simple result of the blood pressure waveform of the ascending aorta, its utility in clinical decision-making is sufficiently validated [52, 54, 55]. The SEVR is not limited to hearts with normal structures. We investigated SEVR in patients after the Norwood procedure, which reconstructs the ascending aorta using the pulmonary trunk and native aorta [54]. In our cohort without aortopulmonary shunts, SEVR was markedly lower than

Fig. 8.3 (continued) Lower panel: Descending aortic pressure waveform in a patient with a normal aortic arch. The interval between upstroke and Ri in the descending aorta is shorter than that of the ascending aorta, with systolic pressure higher than that of the ascending aorta. High pressure is suitable for preserving potential energy in the aortic elastic fiber to effectively deliver blood to the peripheral organ. (**b**) *Upper panel*: Ascending aortic pressure waveform in a patient who underwent the Norwood procedure. There were two possible inflection points. The first inflection represented the reflection from proximal impedance mismatch, which heightened early systolic pressure. The second reflection wave appeared to be derived from the distal part of the aorta. Lower panel: Descending aortic pressure waveform in a patient who underwent a Norwood procedure. In contrast to Fig. 8.3a, peak aortic pressure was biased to the late systolic phase, which resulted in less systolic pressure. This means impaired preservation of potential energy in the aorta

that of control patients with neither significant heart disease nor aortopulmonary shunt in whom all pulmonary blood flow was supplied from the aorta (Fig. 8.4). Accordingly, we concluded that post-Norwood aortas predisposed patients to being more susceptible to coronary ischemia, even without significant coronary stenosis. In this study, aortic impedance mismatch, as was represented by descending aortic relative narrowing compared to that in the ascending aorta, was a significant determinant of SEVR. Furthermore, SEVR was negatively correlated with the renin–angiotensin–aldosterone system and natriuretic peptides (atrial natriuretic peptide [ANP] and brain natriuretic peptide [BNP]), suggesting a promising marker for fibrosis or heart failure. This was further supported by the fact that patient outcome was also associated with SEVR. Our novel finding regarding the role of SEVR emphasizes the importance of guiding proper aortic reconstruction in hypoplastic left heart syndrome, and this might be extrapolated to other congenital heart diseases. The aortic reservoir function in the TOF with aortopathy is expected to be decreased. Although impaired coronary perfusion reserve in patients with decreased aortic distensibility was identified using simultaneous measures of aortic and coronary pressure/flow [56], the possibility that SEVR might also detect similar myocardial blood flow demand–supply imbalances as well as late complications, such as arrhythmias, will be further investigated.

8.4.4 Estimation of Aortic Volume Flow

As mentioned, aortic blood flow velocity is closely related to shear stress. Guzzardi et al. investigated aortopathy patients using MR flow mapping and actual aortic

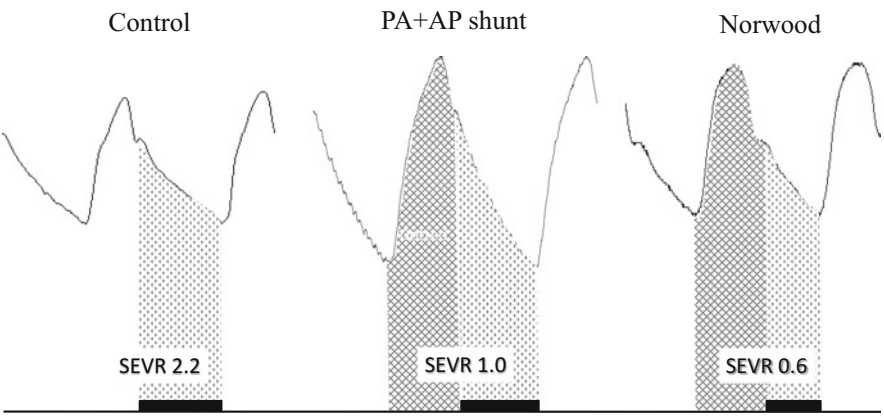

Fig. 8.4 Anatomical features of the subendocardial viability ratio. Mesh area, tension time index (TTI); dotted area, diastolic time index (DTI); filled area, pressure time integral of systemic ventricle. The ratio of DTI to TTI denotes the subendocardial viability ratio (SEVR). SEVR in a patient who underwent the Norwood procedure (RV-PA conduit) was significantly lower than that of controls and even lower than that of patients with pulmonary atresia plus aortopulmonary shunt

wall tissue sampled during surgery, and they elucidated that TGF-β1 and its downstream matrix metalloproteinases are upregulated in the aortic wall exposed to high shear stress but less so in the aortic wall, where less shear stress was observed [12]. Despite the advantages of MRI, which accurately assesses blood flow velocity at a specific location, heart rate variability due to room temperature, the small number of available beats for assessments, and existence of turbulence flow (i.e., pressure recovery in aortic stenosis) are limiting factors for obtaining clinically relevant aortic volume flow. Using cardiac catheterization, the Fick formula also allows us to estimate net aortic blood flow regardless of hemodynamic characteristics or existence of arrhythmias. Although available aortic flow, flow velocity, and shear stress itself cannot be directly estimated using the Fick method, they represent averaged volume loading to the aorta. Our previous data and those of others suggest the significant impact of aortic volume loading on the development of aortic dilatation [5, 6, 13].

The use of simultaneous Doppler flow and pressure wire further allow us to obtain actual blood flow velocity in a beat-by-beat manner with simultaneous measurements of the pressure waveform. Having both the pressure and flow waveforms allows us to factorize pressure/flow waveforms into forward (cardiac contribution) and backward (reflection) flow [44, 57]. The existence of backward flow that overlaps the systolic pressure is attributable to augmented ventricular pulsatile afterload. Accordingly, identifying backward flow and avoiding overlap of the upslope of forward pressure flow by pharmacological intervention will contribute to better management of aortopathy. Westerhof et al. reported the possibility of factorizing the pressure waveform into forward and backward pressure without measuring the flow waveform, but further validation is needed [45].

8.4.5 Cardiac Property

Progression of aortopathy implies afterload increase as well as coronary circulatory insufficiency [9, 21, 51]. Because both affect cardiac performance and geometry [9, 47], assessments of cardiac properties and ventricular–arterial coupling should be considered fundamental constituents of physiology in aortopathy. Venous congestion, which is often accompanied by heart failure, is known to predispose to fibrogenesis and inflammation [58]; therefore, coexistence of cardiac malfunction may accelerate aortic degradation. Using ventricular pressure and simultaneous ventricular volume measurements, the ventricular pressure–volume loop can be constructed either in structurally normal hearts or in those with congenital heart diseases (Fig. 8.5) [59–61]. Load-independent measurements for cardiac contractility (end-systolic pressure–volume relationship [ESPVR]) and diastolic passive stiffness (end-diastolic pressure–volume relationship [EDPVR]) can be determined, and those data allow us to determine therapeutic targets of hemodynamics to improve cardiac function or metabolism [62]. The ratio of end-systolic elastance (Ees) to arterial elastance (Ea) provides VA coupling (Ees/Ea), which is the

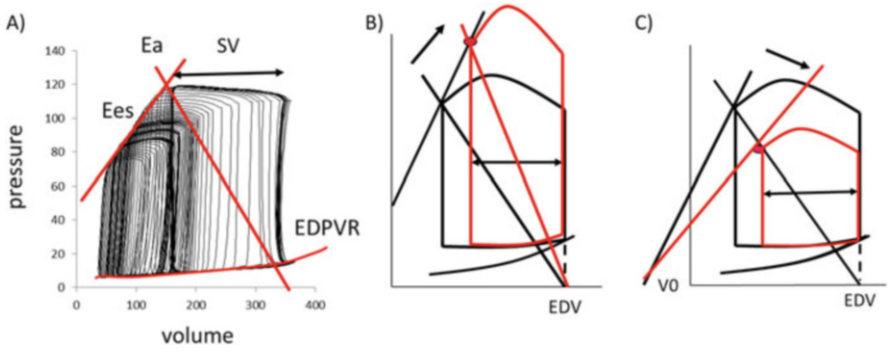

Fig. 8.5 Pressure–volume relationship of the ventricle. *Ea* effective arterial elastance, *Ees* end-systolic elastance, *EDPVR* end-diastolic pressure–volume relationship, *EDV* end-diastolic volume, *SV* stroke volume. (**a**) Pressure–volume relationship. Each loop represents the ventricular pressure–volume relationship during volume reduction (IVC occlusion), and the width of each loop represents stroke volume (SV). Ventricular pressure and volume at end systole construct a straight slope, and the end-systolic pressure–volume relationship (ESPVR) and its slope are called the end-systolic elastance (Ees), a load-independent measurement of ventricular contractility. Effective arterial elastance (Ea), a measurement of ventricular afterload, is calculated as the end-systolic pressure divided by the SV. The ventricular diastolic property is characterized by the slope of the pressure–volume relationship of the end diastole (end-diastolic pressure–volume relationship [EDPVR]). (**b**) Increase of afterload. Aortic stiffening augments the ventricular pulsatile load. Stroke volume declines with the increase of afterload (Red). Even without suppression of Ees, the increase of Ea reduces the Ees/Ea ratio; therefore, ventricular efficiency declines and cardiac energetic consumption increases (pressure–volume area↑). (**c**) Impaired cardiac contractility. Due to aortopathy and aortic stiffness, coronary perfusion can be suppressed; therefore, the decline of contractility (Ees↓) and the decline of SV can occur

measure of cardiac performance in relation to afterload [63]. Both ESPVR and coupling ratio (Ees/Ea) are associated with ventricular oxygen consumption in an experimental model [30]. As discussed in the previous section, myocardial circulation in the aortopathy might be impaired, so an energy-preserving strategy might be needed in cases in which unfavorable ventricular energetics is identified. Although aortopathy and ventricular stiffening appear to relate to ventricular diastolic properties, as was suggested by the close relationship between E/e′ and AI in the work by Lee et al. [47], they could not verify how relaxation or passive stiffness relates to arterial property. In addition, the utility of E/e′ was not fully validated in congenital heart diseases [64]; accordingly, more accurate and validated assessments of ventricular diastolic function further support the use of catheter assessment. Accumulating evidence suggests that the coronary microvasculature might be responsible for ventricular diastolic stiffness [65, 66]. In addition to innate cardiac function, external force derived from the pericardium or right ventricle can affect left ventricular preload and stroke volume, which can also be identified by the pressure–volume relationship during right ventricular unloading [67]. While high ventricular diastolic pressure derived from right ventricular dilatation or ventricular stiffening can hinder coronary circulation by decreasing

the aorto-ventricular pressure gradient in the diastole, an increase of the RV load demands more coronary flow [68], causing a coronary supply–demand imbalance. Together, PV loops allow us to identify the issues predisposing to cardiac dysfunction coupled with aortopathy. Ventricular mechanics in patients with aortopathy is not well recognized, particularly when there is additional ventricular load. Further investigation is warranted in this field.

8.4.6 Possible Role of Impedance Analysis

Although PWV and aortic waveforms (AI) are simple but reliable indexes of aortic properties and impedance mismatch, they are relatively sensitive to blood pressure, aortic caliber change, and heart rate. Plenty of evidence that relates aortopathy to its fundamental constituents of focal aortic stiffening is available using PWV or AI; therefore, the additive role of relatively load-independent measurements of vascular properties, such as input impedance, may not be particularly needed in clinical practice. However, advances in noninvasive technology for measuring pressure and flow waveforms in the ascending aorta may expand the utility of input impedance for the management or better understanding of aortopathy.

Impedance denotes the sum of all types of opposition, which is confined to oscillatory motion (alternating current) to blood flow distal to the measurement site in the cardiovascular circuit. Whereas a few types of impedance (longitudinal impedance, input impedance, characteristic impedance, terminal impedance) are defined in the arterial system, input impedance, which defines the relationship between pulsatile flow and pulsatile pressure provided to the particular vascular system, is commonly used in cardiovascular research. Similar to the electrical circuit, it denotes the transfer function between blood flow and pressure waveforms. Impedance can be calculated using simultaneous measurements of blood flow and pressure waveforms at any site of the vessel. Advantages of having input impedance are the feature of comprehensive assessment in the entire vascular system distal to the measurement site (thus, resistance, characteristic impedance, and reflection coefficient can be evaluated at the same time) [27, 33] and relative independence of the caliber change or vascular wall thickness (includes segmental change of vascular property). Input impedance can be factorized into each harmonic property, where each harmonic represents a relatively specific vascular property, including proximal, distal, or pulsatile load. Taking advantage of this feature, the impedance of aortopathy can be evaluated regardless of stenosis or dilatation. In previous publications, aortic impedance in patients with Marfan syndrome was investigated in relation to aortic dilatation. Interestingly, most of the study concluded that the aortic characteristic impedance and reflection coefficient of Marfan syndrome were normal, even though aortic dilatation was significant [69, 70]. Assuming aortic dilatation is the result of compensation to maintain aortic impedance within a normal range under the condition of augmented aortic stiffness [10], analyses in these studies were cross-sectional; therefore, impedance analysis may still provide

a predictive value for future development of aortopathy in Marfan syndrome and possibly other diseases susceptible to aortopathy. We evaluated pulmonary arterial properties in TOF patients utilizing input impedance and revealed that impedance at a fundamental frequency and pulmonary arterial compliance were significantly correlated with right ventricular eccentric hypertrophy [71]. We also found increased aortic input impedance in postoperative TOF patients. Increased impedance was associated with increased aortic diameter and reduced left ventricular ejection [72].

8.5 Conclusions

As reviewed in this chapter, catheter examination provides indispensable information regarding vascular properties of aortopathy even more so than advanced imaging modalities. Although the indication for catheter insertion in patients with a fragile aortic wall needs to be considered carefully, the assessments we introduced here are recommended for patients with congenital heart diseases who are at risk for aortopathy. Those patients require catheter examinations often for perioperative assessment and/or catheter interventions, so they have more opportunities for the insertion of catheters. In addition, hemodynamic assessments performed using catheters are the gold standard that is necessary to verify the appropriateness of noninvasive images, including echocardiograms or MRI scans. Extensive knowledge regarding hemodynamics is required for maximizing catheter examinations as the standard for hemodynamic assessments that contribute robust evidence regarding aortopathy. The goal of this chapter is to help others understand hemodynamics in aortopathy.

References

1. Cheng HM, Lang D, Tufanaru C, Pearson A (2013) Measurement accuracy of non-invasively obtained central blood pressure by applanation tonometry: a systematic review and meta-analysis. Int J Cardiol 167:1867–1876
2. Delles M, Rengier F, Jeong YJ, von Tengg-Kobligk H, Ley S, Kauczor HU, Dillmann R, Unterhinninghofen R (2013) Estimation of aortic pressure waveforms from 4d phase-contrast mri. Conf Proc IEEE Eng Med Biol Soc 2013:731–734
3. Tan JL, Davlouros PA, McCarthy KP, Gatzoulis MA, Ho SY (2005) Intrinsic histological abnormalities of aortic root and ascending aorta in tetralogy of fallot: evidence of causative mechanism for aortic dilatation and aortopathy. Circulation 112:961–968
4. Niwa K, Perloff JK, Bhuta SM, Laks H, Drinkwater DC, Child JS, Miner PD (2001) Structural abnormalities of great arterial walls in congenital heart disease: light and electron microscopic analyses. Circulation 103:393–400
5. Seki M, Kurishima C, Kawasaki H, Masutani S, Senzaki H (2012) Aortic stiffness and aortic dilation in infants and children with tetralogy of fallot before corrective surgery: evidence for intrinsically abnormal aortic mechanical property. Eur J cardiothorac Surg 41:277–282

6. de Simone G, Roman MJ, De Marco M, Bella JN, Izzo R, Lee ET, Devereux RB (2015) Hemodynamic correlates of abnormal aortic root dimension in an adult population: the strong heart study. J Am Heart Assoc 4
7. Girdauskas E, Borger MA, Secknus MA, Girdauskas G, Kuntze T (2011) Is aortopathy in bicuspid aortic valve disease a congenital defect or a result of abnormal hemodynamics? A critical reappraisal of a one-sided argument. Eur J cardiothorac Surg 39:809–814
8. Shim CY, Cho IJ, Yang WI, Kang MK, Park S, Ha JW, Jang Y, Chung N (2011) Central aortic stiffness and its association with ascending aorta dilation in subjects with a bicuspid aortic valve. J Am Soc Echocardiogr 24:847–852
9. Grotenhuis HB, Ottenkamp J, Westenberg JJ, Bax JJ, Kroft LJ, de Roos A (2007) Reduced aortic elasticity and dilatation are associated with aortic regurgitation and left ventricular hypertrophy in nonstenotic bicuspid aortic valve patients. J Am Coll Cardiol 49:1660–1665
10. Jeremy RW, Robertson E, Lu Y, Hambly BD (2013) Perturbations of mechanotransduction and aneurysm formation in heritable aortopathies. Int J Cardiol 169:7–16
11. Kim YG, Sun BJ, Park GM, Han S, Kim DH, Song JM, Kang DH, Song JK (2012) Aortopathy and bicuspid aortic valve: haemodynamic burden is main contributor to aortic dilatation. Heart 98:1822–1827
12. Guzzardi DG, Barker AJ, van Ooij P, Malaisrie SC, Puthumana JJ, Belke DD, Mewhort HE, Svystonyuk DA, Kang S, Verma S, Collins J, Carr J, Bonow RO, Markl M, Thomas JD, McCarthy PM, Fedak PW (2015) Valve-related hemodynamics mediate human bicuspid aortopathy: insights from wall shear stress mapping. J Am Coll Cardiol 66:892–900
13. Altit G, Sarquella-Brugada G, Dahdah N, Dallaire F, Carceller AM, Abadir S, Fournier A (2014) Effect of dual-chamber pacemaker implantation on aortic dilatation in patients with congenital heart block. Am J Cardiol 114:1573–1577
14. Sherratt MJ (2009) Tissue elasticity and the ageing elastic fibre. Age (Dordr) 31:305–325
15. Segura AM, Luna RE, Horiba K, Stetler-Stevenson WG, McAllister HA Jr, Willerson JT, Ferrans VJ (1998) Immunohistochemistry of matrix metalloproteinases and their inhibitors in thoracic aortic aneurysms and aortic valves of patients with marfan's syndrome. Circulation 98:II331–II337 discussion II337–338
16. Grewal N, Gittenberger-de Groot AC, DeRuiter MC, Klautz RJ, Poelmann RE, Duim S, Lindeman JH, Koenraadt WM, Jongbloed MR, Mohamed SA, Sievers HH, Bogers AJ, Goumans MJ (2014) Bicuspid aortic valve: phosphorylation of c-kit and downstream targets are prognostic for future aortopathy. Eur J cardiothorac Surg 46:831–839
17. Dietz HC, Pyeritz RE, (1995) Mutations in the human gene for fibrillin-1 (fbn 1) in the marfan syndrome and related disorders. Hum Mol Genet 4 Spec No: 1799–1809
18. Snow HM, Markos F, O'Regan D, Pollock K (2001) Characteristics of arterial wall shear stress which cause endothelium-dependent vasodilatation in the anaesthetized dog. J Physiol 531:843–848
19. Drexler H, Zeiher AM, Wollschlager H, Meinertz T, Just H, Bonzel T (1989) Flow-dependent coronary artery dilatation in humans. Circulation 80:466–474
20. Kang H, Cancel LM, Tarbell JM (2014) Effect of shear stress on water and ldl transport through cultured endothelial cell monolayers. Atherosclerosis 233:682–690
21. Senzaki H, Iwamoto Y, Ishido H, Matsunaga T, Taketazu M, Kobayashi T, Asano H, Katogi T, Kyo S (2008) Arterial haemodynamics in patients after repair of tetralogy of fallot: influence on left ventricular after load and aortic dilatation. Heart 94:70–74
22. Stefanadis C, Vlachopoulos C, Karayannacos P, Boudoulas H, Stratos C, Filippides T, Agapitos M, Toutouzas P (1995) Effect of vasa vasorum flow on structure and function of the aorta in experimental animals. Circulation 91:2669–2678
23. Angouras D, Sokolis DP, Dosios T, Kostomitsopoulos N, Boudoulas H, Skalkeas G, Karayannacos PE (2000) Effect of impaired vasa vasorum flow on the structure and mechanics of the thoracic aorta: implications for the pathogenesis of aortic dissection. Eur J cardiothorac Surg 17:468–473

24. Khono K, Tamai A, Kobayashi T, Senzaki H (2011) Effects of stent implantation for peripheral pulmonary artery stenosis on pulmonary vascular hemodynamics and right ventricular function in a patient with repaired tetralogy of fallot. Heart Vessel 26:672–676
25. Dobson G, Flewitt J, Tyberg JV, Moore R, Karamanoglu M (2006) Endografting of the descending thoracic aorta increases ascending aortic input impedance and attenuates pressure transmission in dogs. Eur J cardiothorac Surg 32:129–135
26. Senzaki H, Masutani S, Kobayashi J, Kobayashi T, Sasaki N, Asano H, Kyo S, Yokote Y, Ishizawa A (2002) Ventricular afterload and ventricular work in fontan circulation: comparison with normal two-ventricle circulation and single-ventricle circulation with blalock-taussig shunts. Circulation 105:2885–2892
27. Senzaki H, Chen CH, Ishido H, Masutani S, Matsunaga T, Taketazu M, Kobayashi T, Sasaki N, Kyo S, Yokote Y (2005) Arterial hemodynamics in patients after kawasaki disease. Circulation 111:2119–2125
28. Sedaghat S, Mattace-Raso FU, Hoorn EJ, Uitterlinden AG, Hofman A, Ikram MA, Franco OH, Dehghan A (2015) Arterial stiffness and decline in kidney function. Clin J Am Soc Nephrol 10 (12):2190–2197
29. Cooper LL, Woodard T, Sigurdsson S, van Buchem MA, Torjesen AA, Inker LA, Aspelund T, Eiriksdottir G, Harris TB, Gudnason V, Launer LJ, Mitchell GF (2015) Cerebrovascular damage mediates relations between aortic stiffness and memory. Hypertension 67(1):176–182
30. Burkhoff D, Sagawa K (1986) Ventricular efficiency predicted by an analytical model. Am J Phys 250:R1021–R1027
31. Senzaki H, Iwamoto Y, Ishido H, Masutani S, Taketazu M, Kobayashi T, Katogi T, Kyo S (2008) Ventricular-vascular stiffening in patients with repaired coarctation of aorta: integrated pathophysiology of hypertension. Circulation 118:S191–S198
32. Townsend RR, Wilkinson IB, Schiffrin EL, Avolio AP, Chirinos JA, Cockcroft JR, Heffernan KS, Lakatta EG, McEniery CM, Mitchell GF, Najjar SS, Nichols WW, Urbina EM, Weber T (2015) Recommendations for improving and standardizing vascular research on arterial stiffness: a scientific statement from the american heart association. Hypertension 66:698–722
33. Saiki H, Senzaki H (2015) Congenital heart disease: morphological and functional assessment chapter 6. Springer, Heidelberg
34. Kim J, Song TJ, Song D, Lee KJ, Kim EH, Lee HS, Nam CM, Nam HS, Kim YD, Heo JH (2014) Brachial-ankle pulse wave velocity is a strong predictor for mortality in patients with acute stroke. Hypertension 64:240–246
35. Regnault V, Lagrange J, Pizard A, Safar ME, Fay R, Pitt B, Challande P, Rossignol P, Zannad F, Lacolley P (2014) Opposite predictive value of pulse pressure and aortic pulse wave velocity on heart failure with reduced left ventricular ejection fraction: Insights from an eplerenone post-acute myocardial infarction heart failure efficacy and survival study (ephesus) substudy. Hypertension 63:105–111
36. Reed CM, Fox ME, Alpert BS (1993) Aortic biomechanical properties in pediatric patients with the marfan syndrome, and the effects of atenolol. Am J Cardiol 71:606–608
37. Nollen GJ, Groenink M, Tijssen JG, Van Der Wall EE, Mulder BJ (2004) Aortic stiffness and diameter predict progressive aortic dilatation in patients with marfan syndrome. Eur Heart J 25:1146–1152
38. Warner PJ, Al-Quthami A, Brooks EL, Kelley-Hedgepeth A, Patvardhan E, Kuvin JT, Heffernan KS, Huggins GS (2013) Augmentation index and aortic stiffness in bicuspid aortic valve patients with non-dilated proximal aortas. BMC Cardiovasc Disord 13:19
39. Seki M, Kurishima C, Saiki H, Masutani S, Arakawa H, Tamura M, Senzaki H (2014) Progressive aortic dilation and aortic stiffness in children with repaired tetralogy of fallot. Heart Vessel 29:83–87
40. Kojima T, Kuwata S, Kurishima C, Iwamoto Y, Saiki H, Ishido H, Masutani S, Senzaki H (2014) Aortic root dilatation and aortic stiffness in patients with single ventricular circulation. Circ J 78:2507–2511

41. Nakagawa R, Kuwata S, Kurishima C, Saiki H, Iwamoto Y, Sugimoto M, Ishido H, Masutani S, Senzaki H (2015) Arterial stiffness in patients after kawasaki disease without coronary artery involvement: Assessment by performing brachial ankle pulse wave velocity and cardio-ankle vascular index. J Cardiol 66:130–134
42. Saiki H, Kurishima C, Masutani S, Senzaki H (2014) Cerebral circulation in patients with fontan circulation: assessment by carotid arterial wave intensity and stiffness. Ann Thorac Surg 97:1394–1399
43. Saiki H, Kojima T, Seki M, Masutani S, Senzaki H (2012) Marked disparity in mechanical wall properties between ascending and descending aorta in patients with tetralogy of fallot. Eur J cardiothorac Surg 41:570–573
44. Westerhof N, Sipkema P, van den Bos GC, Elzinga G (1972) Forward and backward waves in the arterial system. Cardiovasc Res 6:648–656
45. Westerhof BE, Guelen I, Westerhof N, Karemaker JM, Avolio A (2006) Quantification of wave reflection in the human aorta from pressure alone: a proof of principle. Hypertension 48:595–601
46. Sakurai M, Yamakado T, Kurachi H, Kato T, Kuroda K, Ishisu R, Okamoto S, Isaka N, Nakano T, Ito M (2007) The relationship between aortic augmentation index and pulse wave velocity: an invasive study. J Hypertens 25:391–397
47. Lee SY, Shim CY, Hong GR, Seo J, Cho I, Cho IJ, Chang HJ, Ha JW, Chung N (2015) Association of aortic phenotypes and mechanical function with left ventricular diastolic function in subjects with normally functioning bicuspid aortic valves and comparison to subjects with tricuspid aortic valves. Am J Cardiol 116:1547–1554
48. Murakami T, Shirai T, Shiina Y, Niwa K (2015) Compression of superior caval vein - new clinical problem of aortopathy. Int J Cardiol 191:235–236
49. Saiki H, Sugimoto M, Kuwata S, Kurishima C, Iwamoto Y, Ishido H, Masutani S, Senzaki H (2015) Novel mechanisms for cerebral blood flow regulation in patients with congenital heart disease. Am Heart J 172:152–159
50. Tsao CW, Lyass A, Larson MG, Levy D, Hamburg NM, Vita JA, Benjamin EJ, Mitchell GF, Vasan RS (2015) Relation of central arterial stiffness to incident heart failure in the community. J Am Heart Assoc 4(11):e002189
51. Nobari S, Mongrain R, Gaillard E, Leask R, Cartier R (2012) Therapeutic vascular compliance change may cause significant variation in coronary perfusion: a numerical study. Comput Math Methods Med 2012:791686
52. Brazier J, Cooper N, Buckberg G (1974) The adequacy of subendocardial oxygen delivery: the interaction of determinants of flow, arterial oxygen content and myocardial oxygen need. Circulation 49:968–977
53. Buckberg GD, Fixler DE, Archie JP, Hoffman JI (1972) Experimental subendocardial ischemia in dogs with normal coronary arteries. Circ Res 30:67–81
54. Saiki H, Kuwata S, Kurishima C, Masutani S, Senzaki H (2016) Vulnerability of coronary circulation after norwood operation. Ann Thorac Surg 101(4):1544–1551
55. Tsiachris D, Tsioufis C, Syrseloudis D, Roussos D, Tatsis I, Dimitriadis K, Toutouzas K, Tsiamis E, Stefanadis C (2012) Subendocardial viability ratio as an index of impaired coronary flow reserve in hypertensives without significant coronary artery stenoses. J Hum Hypertens 26:64–70
56. Ohtsuka S, Kakihana M, Watanabe H, Sugishita Y (1994) Chronically decreased aortic distensibility causes deterioration of coronary perfusion during increased left ventricular contraction. J Am Coll Cardiol 24:1406–1414
57. Murgo JP, Westerhof N, Giolma JP, Altobelli SA (1981) Manipulation of ascending aortic pressure and flow wave reflections with the valsalva maneuver:relationship to input impedance. Circulation 63:122–132
58. Colombo PC, Onat D, Harxhi A, Demmer RT, Hayashi Y, Jelic S, LeJemtel TH, Bucciarelli L, Kebschull M, Papapanou P, Uriel N, Schmidt AM, Sabbah HN, Jorde UP (2014) Peripheral

venous congestion causes inflammation, neurohormonal, and endothelial cell activation. Eur Heart J 35:448–454
59. Senzaki H, Masutani S, Ishido H, Taketazu M, Kobayashi T, Sasaki N, Asano H, Katogi T, Kyo S, Yokote Y (2006) Cardiac rest and reserve function in patients with fontan circulation. J Am Coll Cardiol 47:2528–2535
60. Suga H, Sagawa K (1974) Instantaneous pressure-volume relationships and their ratio in the excised, supported canine left ventricle. Circ Res 35:117–126
61. Kass DA, Maughan WL (1988) From 'emax' to pressure-volume relations: a broader view. Circulation 77:1203–1212
62. Burkhoff D, Mirsky I, Suga H (2005) Assessment of systolic and diastolic ventricular properties via pressure-volume analysis: a guide for clinical, translational, and basic researchers. Am J Physiol Heart Circ Physiol 289:H501–H512
63. Senzaki H, Kyo S, Matsumoto K, Asano H, Masutani S, Ishido H, Matunaga T, Taketatu M, Kobayashi T, Sasaki N, Yokote Y (2004) Cardiac resynchronization therapy in a patient with single ventricle and intracardiac conduction delay. J Thorac Cardiovasc Surg 127:287–288
64. Masutani S, Saiki H, Kurishima C, Kuwata S, Tamura M, Senzaki H (2014) Assessment of ventricular relaxation and stiffness using early diastolic mitral annular and inflow velocities in pediatric patients with heart disease. Heart Vessel 29:825–833
65. Mohammed SF, Hussain S, Mirzoyev SA, Edwards WD, Maleszewski JJ, Redfield MM (2015) Coronary microvascular rarefaction and myocardial fibrosis in heart failure with preserved ejection fraction. Circulation 131:550–559
66. Paulus WJ, Tschope C (2013) A novel paradigm for heart failure with preserved ejection fraction: Comorbidities drive myocardial dysfunction and remodeling through coronary microvascular endothelial inflammation. J Am Coll Cardiol 62:263–271
67. Dauterman K, Pak PH, Maughan WL, Nussbacher A, Arie S, Liu CP, Kass DA (1995) Contribution of external forces to left ventricular diastolic pressure. Implications for the clinical use of the starling law. Ann Intern Med 122:737–742
68. Aburawi EH, Munkhammar P, Carlsson M, El-Sadig M, Pesonen E (2014) Coronary flow dynamics in children after repair of tetralogy of fallot. Int J Cardiol 172:122–126
69. Yin FC, Brin KP, Ting CT, Pyeritz RE (1989) Arterial hemodynamic indexes in marfan's syndrome. Circulation 79:854–862
70. Segers P, De Backer J, Devos D, Rabben SI, Gillebert TC, Van Bortel LM, De Sutter J, De Paepe A, Verdonck PR (2006) Aortic reflection coefficients and their association with global indexes of wave reflection in healthy controls and patients with marfan's syndrome. Am J Physiol Heart Circ Physiol 290:H2385–H2392
71. Inuzuka R, Seki M, Sugimoto M, Saiki H, Masutani S, Senzaki H (2013) Pulmonary arterial wall stiffness and its impact on right ventricular afterload in patients with repaired tetralogy of fallot. Ann Thorac Surg 96:1435–1441
72. Senzaki H, Iwamoto Y, Ishido H, Matsunaga T, Taketazu M, Kobayashi T, Asano H, Katogi T, Kyo S (2007) Arterial hemodynamics in patients after repair of tetralogy of fallot: Influence on left ventricular afterload and aortic dilation. Heart
73. Kelly R, Hayward C, Avolio A, O'Rourke M (1989) Noninvasive determination of age-related changes in the human arterial pulse. Circulation 80:1652–1659